Chemical Science

ROYAL SOCIETY OF CHEMISTRY

EDGE ARTICLE

View Article Online
View Journal | View Issue

Cite this: *Chem. Sci.*, 2020, **11**, 10119

All publication charges for this article have been paid for by the Royal Society of Chemistry

Received 18th May 2020
Accepted 6th September 2020

DOI: 10.1039/d0sc02828b

rsc.li/chemical-science

Asymmetric allylic substitution–isomerization to axially chiral enamides *via* hydrogen-bonding assisted central-to-axial chirality transfer†

Chao Sun,‡[a] Xiaotian Qi,‡[b] Xiao-Long Min,[a] Xue-Dan Bai,[a] Peng Liu *[bc] and Ying He *[a]

Axially chiral enamides bearing a N–C axis have been recently studied and were proposed to be valuable chiral building blocks, but a stereoselective synthesis has not been achieved. Here, we report the first enantioselective synthesis of axially chiral enamides *via* a highly efficient, catalytic approach. In this approach, C(sp^2)–N bond formation is achieved through an iridium-catalyzed asymmetric allylation, and then *in situ* isomerization of the initial products through an organic base promoted 1,3-H transfer, leading to the enamide products with excellent central-to-axial transfer of chirality. Computational and experimental studies revealed that the 1,3-H transfer occurs *via* a stepwise deprotonation/re-protonation pathway with a chiral ion-pair intermediate. Hydrogen bonding interactions with the enamide carbonyl play a significant role in promoting both the reactivity and stereospecificity of the stepwise 1,3-H transfer. The mild and operationally simple formal *N*-vinylation reaction delivered a series of configurationally stable axially chiral enamides with good to excellent yields and enantioselectivities.

Introduction

Asymmetric isomerization of allylic compounds has attracted great attention from synthetic chemists due to its 100% atom economy.[1–3] Typical approaches for this transformation are achieved through the transition metal-mediated [1,3]-hydride transfer catalysis. With the development of the area, organic molecule catalysis has enabled efficient enantioselective [1,3]-allylic rearrangements since 2010.[4–13] In this case, [1,3]-H (proton) transfer would occur in the presence of an organic base catalyst. Very recently, the detailed mechanistic studies of stereospecific [1,3]-allylic rearrangements showing chirality transfer were reported by Paton and co-workers.[14] Exemplified by base-catalyzed [1,3]-rearrangement of arylindenols, they proposed that a suprafacial prototopic shift is mediated by the amine base; and the chirality transfer is achieved through a resilient contact ion-pair held together by electrostatic attraction and an NH$\cdots\pi$ interaction (Fig. 1a). Alternatively, cognizant of significant role of hydrogen-bonding interactions in asymmetric olefin isomerization,[15] we were intrigued by the effect of hydrogen-bonding interactions of stereospecific [1,3]-allylic rearrangements.

Recently, we became interested in the construction of axially chiral styrenes. While axially chiral styrenes were proposed as intermediates of interest in the study of chirality transfer decades ago,[16] only recently have strategies for their enantioselective synthesis been disclosed (Fig. 1b).[17–23] Inspired by stereospecific [1,3]-H transfer strategy, we envisioned the preparation of axially chiral styrenes from enantioenriched allylic compounds. *N*-substituted bulky anilide derivatives have attracted much attention as important atropoisomeric compounds with a N–C chiral axis.[24–32] In 2016, Curran and co-workers prepared a collection of axially chiral enamides in racemic form and measured the rate of racemization for chromatographically-separated enantiomers. The authors concluded that, in many cases, enantioenriched enamides are configurationally-stable for periods of days to weeks at room temperature and may serve as building blocks of interest for asymmetric synthesis and construction of molecular gears and machines.[33] Despite their potential applications and inherent interest, access to these compounds remained limited to resolution by chiral chromatography. Catalytic enantioselective synthesis of this new class of axially chiral compounds would constitute a highly desirable synthetic process.

In this scenario, we wondered whether axially chiral enamides could be synthesized *via* stereospecific [1,3]-H transfer. In this case, [1,3]-H transfer would occur *via* a stepwise deprotonation/re-protonation pathway with a chiral ion-pair intermediate. Hydrogen bonding interactions with the enamide carbonyl would play a significant role in promoting both the

[a]School of Chemical Engineering, Nanjing University of Science & Technology, Nanjing 210094, China. E-mail: yhe@njust.edu.cn

[b]Department of Chemistry, University of Pittsburgh, Pittsburgh, Pennsylvania 15260, USA. E-mail: pengliu@pitt.edu

[c]Department of Chemical and Petroleum Engineering, University of Pittsburgh, Pittsburgh, Pennsylvania 15261, USA

† Electronic supplementary information (ESI) available. CCDC 1941459 and 1960857. For ESI and crystallographic data in CIF or other electronic format see DOI: 10.1039/d0sc02828b

‡ These authors contributed equally.

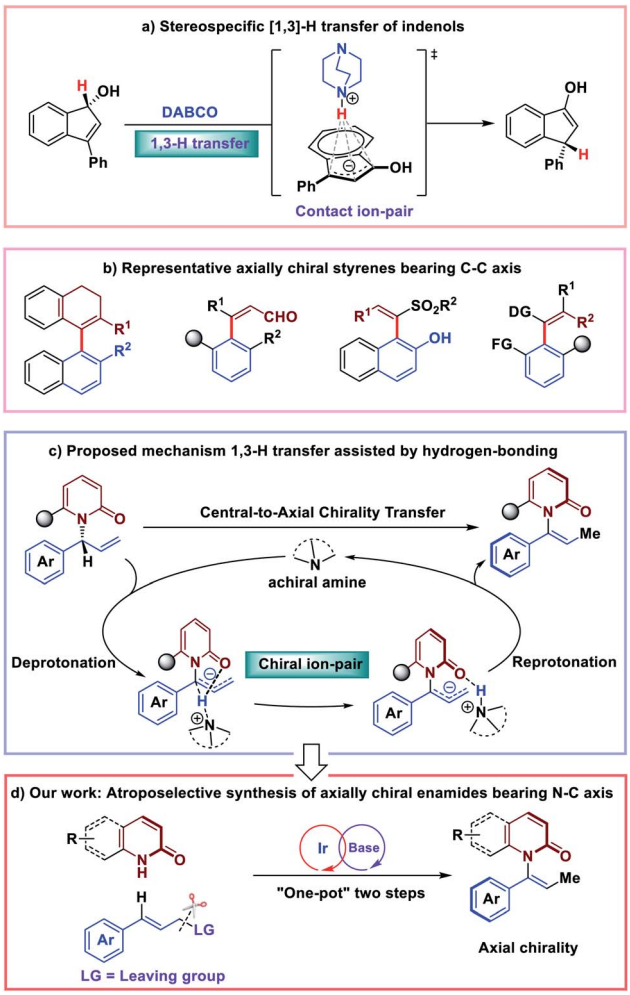

Fig. 1 Central-to-axial chirality transfer inspired by [1,]-H transfer strategy.

reactivity and stereospecificity of the stepwise [1,3]-H transfer (Fig. 1c). More importantly, enantioenriched allylic amides could be easily synthesized by classic iridium-catalyzed asymmetric allylation.[34–42] Due to the basic conditions of the reaction system, we expected that *in situ* isomerization[43,44] of the enantioenriched allylic products by an organic base would lead to the axially chiral enamides *via* "one-pot" two steps process (Fig. 1d).

Nevertheless, at the outset of our studies we anticipated several challenges of finding conditions to achieve our goal of developing a catalytic, enantioselective synthesis of axially-chiral enamides: (1) the products must be obtained with high enantioselectivity, regioselectivity and geometrical (*Z*/*E*) selectivity; (2) the weakly acidic intermediate (more weakly acidic than previously reported substrates for base-mediated chirality transfer) must be deprotonated and re-protonated with high stereochemical fidelity *via* chiral ion pair; and (3) high temperatures and other harsh conditions must be avoided to suppress racemization of the enantioenriched product. Here we report the first catalytic synthesis of axially chiral enamides using a combination of iridium-catalyzed allylation and base-mediated central-to-axial chirality transfer.

Results and discussion

Optimized conditions

With these considerations in mind, we initiated our studies by examining the reaction of cinnamyl carbonate (**1a**) and 2-quinolinol (**2a**) using *in situ* generated iridacycle catalyst (Table 1, see ESI for details†). To our delight, the reaction proceeded smoothly under the "standard conditions", affording the desired product **3a** in 88% yield with 92% ee using **L1** as a ligand (Table 1, entry 1). Upon switching the ligand to **L2–L6** did not yield the product **3a** efficiently (entries 2–6). The use of different bases such as Et_3N, DABCO and TBD led to diminished enantioselectivities and yields (entries 7–9). Examination of solvent effect revealed that compatible yield and enantioselectivity of **3a** was obtained (entries 10 and 11). The leaving groups of **1a** such as –OBz and –Boc led to good enantioselectivities but low yields of 38% and 34%, respectively (entries 12 and 15). A dramatically low ee of −3% and 50% were obtained using –Cl and $-OPO(OEt)_2$ as the leaving group in substrate **1a**.

Table 1 Optimizations of reaction conditions[a]

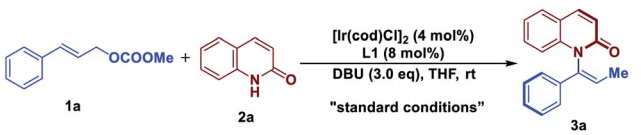

Entry	Variation from standard conditions	ee[b] (%)	Yield[c] (%)
1	None	92	88
2	**L2** instead of **L1** as ligand	—	Trace
3	**L3** instead of **L1** as ligand	13	<5%
4	**L4** instead of **L1** as ligand	—	Trace
5	**L5** instead of **L1** as ligand	−80	—
6	**L6** instead of **L1** as ligand	72	33
7	Et_3N instead of DBU as base	89	33
8	DABCO instead of DBU as base	88	35
9	TBD instead of DBU as base	86	37
10	1,4-dioxane instead of THF as solvent	91	86
11	Toluene instead of THF as solvent	87	64
12	–OBz instead of –OCOOMe	93	38
13	–Cl instead of –OCOOMe	–3	46
14	$-OPO(OEt)_2$ instead of –OCOOMe	50	42
15	–OBoc instead of –OCOOMe	89	34

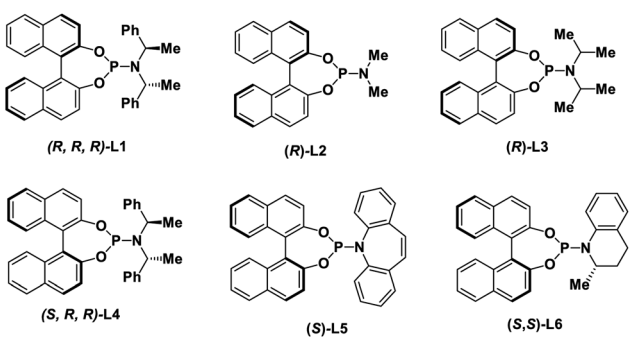

[a] Reaction conditions: all reactions were run on 0.1 mmol scale with respect to **1**. [b] ee determined by chiral HPLC. [c] Isolated yield. DABCO = 1,4-diazabicyclo[2.2.2]octane, DBU = 1,8-diazabicyclo[5.4.0]undec-7-ene, TBD = 1,5,7-triazabicyclo[4.4.0]dec-5-ene.

Substrate Scope of Reaction

With the optimized conditions in hand, we next explored the substrate scope of the reaction (Table 2). In general, C–H amination of a variety of substituted cinnamyl carbonates are well tolerated under optimized conditions. For example, reactions with a range of *para*-substituted cinnamyl carbonates bearing electron-neutral, electron-donating, and electron-withdrawing groups proceeded efficiently to afford the corresponding products in 90–97% ee with 80–95% yield (**3a–3f**). Cinnamyl carbonates containing the *meta*-substituted, electron-poor, and electron-rich substituents also gave us high ee of 90–91% with

Table 2 Substrate scope[a]

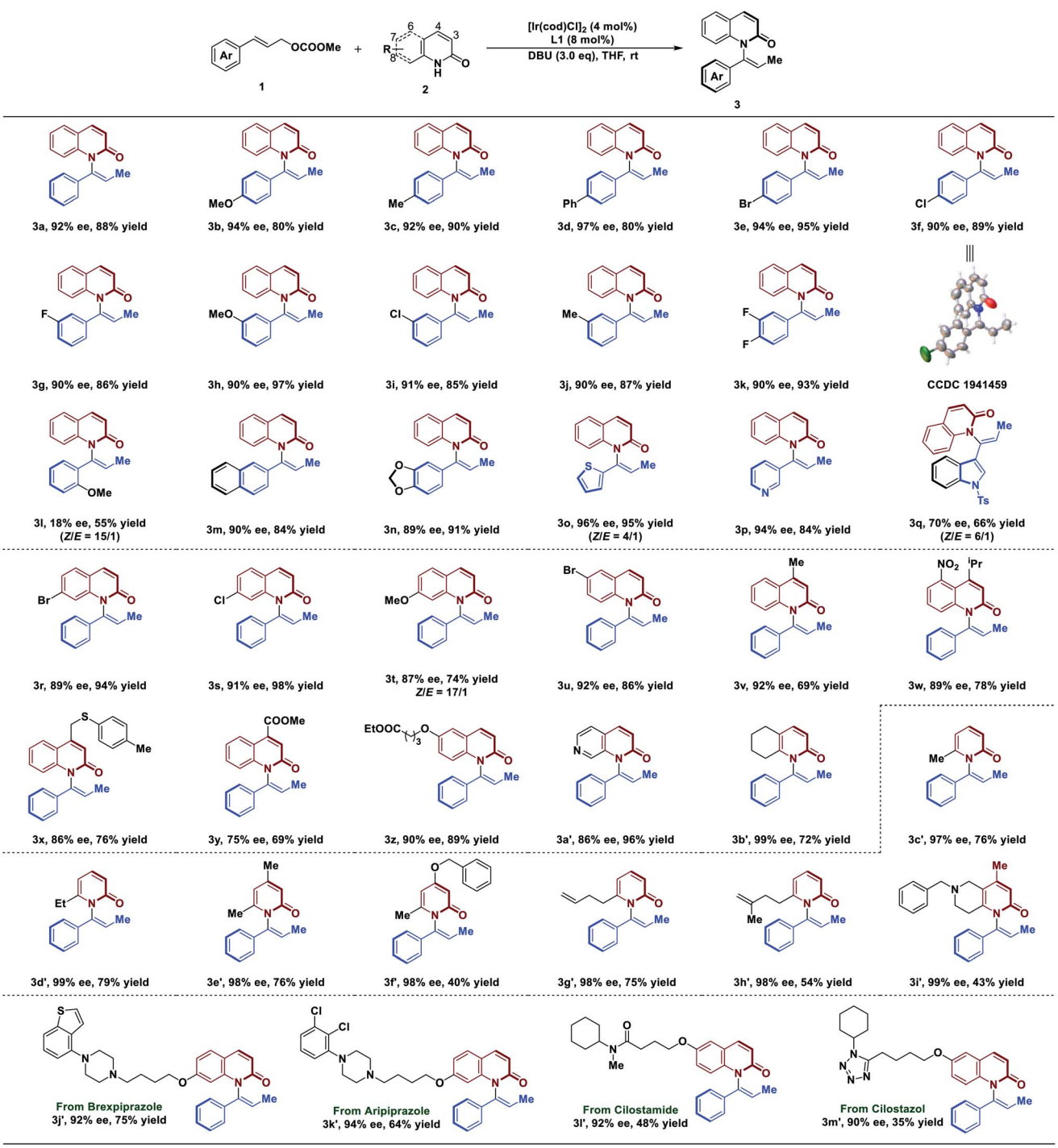

[a] Reaction conditions: all reactions were run on 0.1 mmol scale with respect to **1a**. ee determined by chiral HPLC. Isolated yield. Unless noted, products were obtained with more than 20 : 1 of *Z*/*E*.

85–97% yield (**3g–3j**). Difunctionalized cinnamyl carbonate was compatible with the reaction, leading to the desired product in 90% ee with 93% yield (**3k**). To our disappointment, a lower ee of 18% was obtained using substrate **1** bearing *ortho*-substituent of aryl group (**3l**). Remarkably, reaction tolerated bulky substituent in **1**, affording the desired products in 89–90% ee (**3m** and **3n**). Notably, the reaction was not limited to aryl moieties of substrate **1**; it was also amenable to the heterocyclic rings that afforded the desired products in 94–96% ee with 84–95% yield (**3o** and **3p**). However, the product **3q** was obtained in slightly lower ee (70%) with 66% yield. In addition, the absolute configuration of **3f** was determined by single X-ray crystallographic analysis, and others were assigned by analogy to **3f**.

With respect to 2-quinolinol scope, we investigated the generality of this reaction. As depicted in Table 2, the electronic properties of substituents on 2-quinolinol have a significant effect on the enantioselectivity. Substrates **2** bearing substituents at C8, C7, C6 and C4 positions were well tolerated, affording products in 86–92% ee with 69–98% yield (**3r–3x** and **3z**). However, the use of substrate **2** processing electron-withdrawing group at C4 position gave the product in 75% ee (**3y**). Several 2-quinolinol analogues were then investigated in our catalysis system. Expectedly, the reaction of 2-quinoxalinol with **1a** proceeded readily to afford **3a′** in 86% ee with 96% yield. In addition, the reaction of cinnamyl carbonate with 5,6,7,8-tetrahydroquinolin-2(1*H*)-one resulted in the desired product in 99% ee with 72% yield (**3b′**). Moreover, the reaction is not limited to 2-quinolinol derivatives; substrates such as pyridin-2(1*H*)-one analogues were tolerated, affording the axially chiral enamides **3c′–3f′** in up to 99% ee. It's worth noting that the reaction tolerates the functionalized substrates affording the products **3g′–3i′** in 98–99% ee.

Since quinolinols represent a vital class of heterocyclic units that are extensively utilized in natural products and

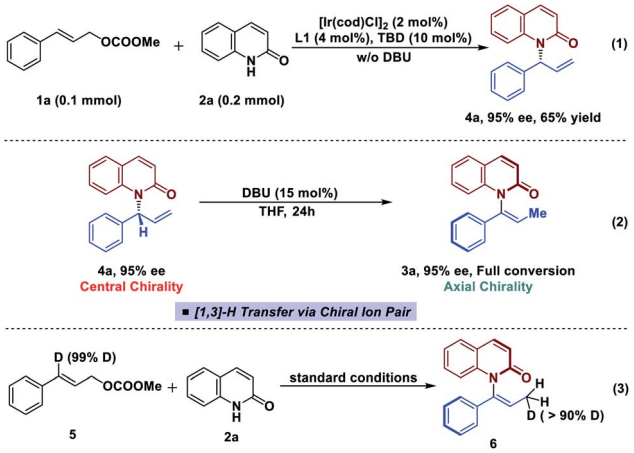

Fig. 2 Control experiments and deuterium labeled experiment.

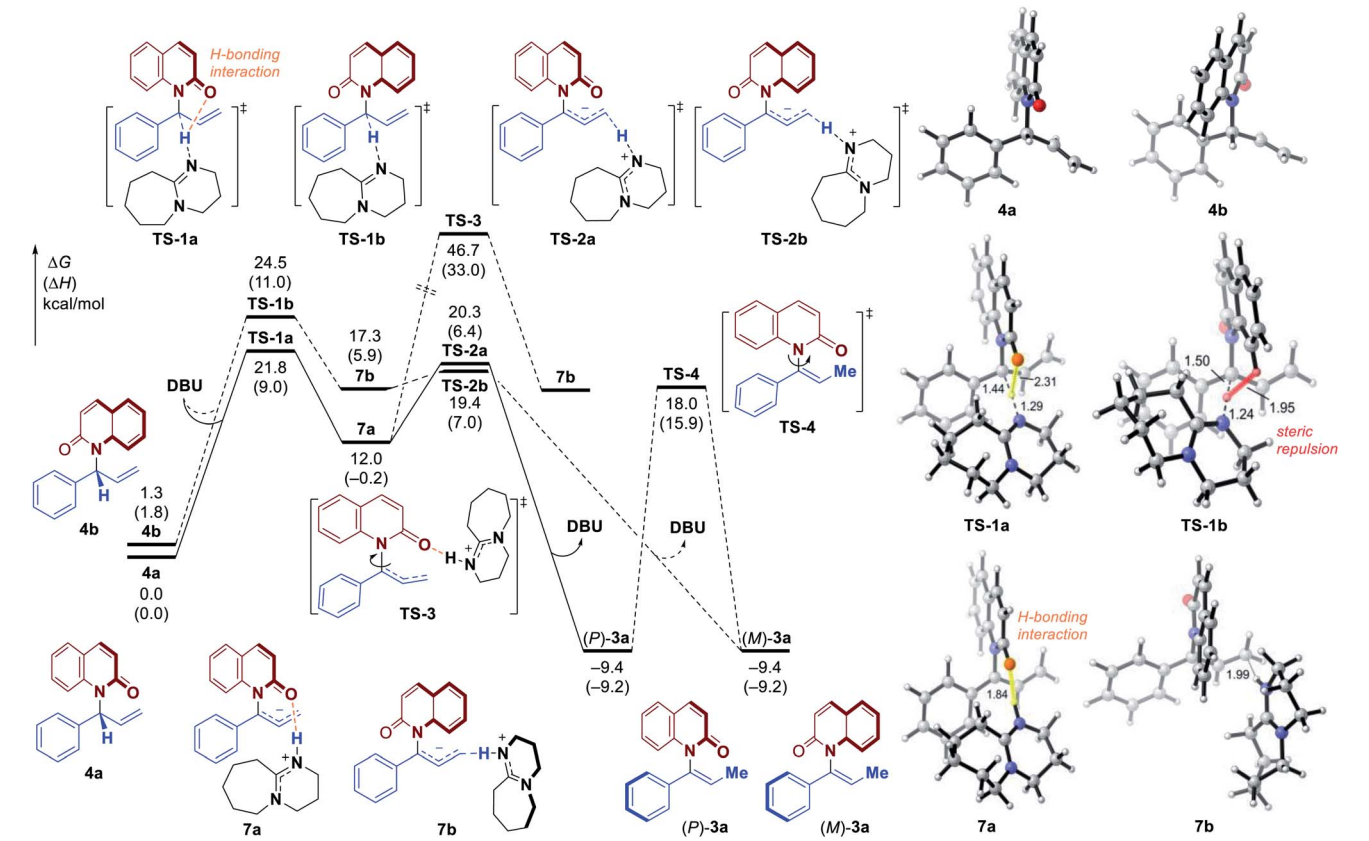

Fig. 3 Free energy profiles of central-to-axial chirality transfer through DBU-promoted [1,]-H transfer. All energies are calculated at M06-2X/6-311++G(d,p)/SMD(THF)//M06-2X/6-31G(d)/SMD(THF) level of theory.

pharmaceuticals,[45–47] decoration of bioactive molecules has been carried out. For example, brexpiprazole and aripiprazole, as antipsychotic medications, are used to treat the symptoms of schizophrenia. Under our conditions, they are readily functionalized to afford **3j′** and **3k′** in 92% ee and 94% ee, respectively. A PDE3 inhibitor, cilostamide, could also undergo atroposelective vinylation to generate axially chiral enamide **3l′** in 92% ee, albeit with 48% yield. The reaction also tolerates a cilostazol derivative which afforded **3m′** in 90% ee. Having established the atroposelective vinylation process for the construction of axially chiral enamides, we next explored the preparative-scale synthesis of product **3a**. As a result, the product was obtained in 91% ee with 73% yield, suggesting that this method has the potential for large-scale chemical production (see ESI for details†).

Mechanistic studies

In an effort to gain more insight into the reaction mechanism, deuterium labeling and control experiments were carried out. To our delight, allylic product **4a** could be obtained by omitting DBU and conducting the reaction using *in situ* generated iridacycle catalyst under near-neutral conditions (Fig. 2, eqn (1)).[48] The subjection of **4a**, isolated in 95% ee, to DBU resulted in efficient and stereospecific isomerization (>99% es) to deliver **3a** in 95% ee with full conversion (eqn (2)); and no isomerization product was obtained in the absence of base. Determination of the absolute stereochemistry of **4a**[49] and **3a** indicated that reprotonation occurred on the face from which deprotonation initially occurred, consistent with a [1,3]-H transfer mechanism involving a contact ion pair (eqn (2), see ESI for details†).[14] High levels of deuterium transfer (>90% D of **6** from 99% D of **5**, eqn (3)) were also consistent with reactions previously proposed that take place through an ion pair intermediate (see ESI for details†).[14]

To further clarify the origin of the high levels of stereospecificity during the central-to-axial chirality transfer, density functional theory (DFT) calculations were performed to study the DBU-promoted [1,3]-H transfer of allylation product **4a** which bears an (*R*)-stereogenic center. As shown in Fig. 3 and 4, [1,3]-H transfer pathways from several conformers of **4a** were considered. The most favorable benzylic C–H deprotonation occurs from the most stable conformer of **4a** *via* transition state **TS-1a** with an activation free energy of 21.8 kcal mol^{-1}. This pathway requires a much lower kinetic barrier than the deprotonation of conformer **4b**, which requires 24.5 kcal mol^{-1} with respect to **4a**. Intrinsic reaction coordinate (IRC) calculation and Born–Oppenheimer molecular dynamics (BOMD) simulation confirmed that this deprotonation transition state leads to a chiral ion-pair intermediate **7a**, which involves strong hydrogen bonding between the iminium N–H and the amide carbonyl group. This N–H···O hydrogen bonding is also observed in the deprotonation transition state (**TS-1a**), as evidenced by a relatively short H···O distance of 2.31 Å. In the deprotonation pathway from conformer **4b** (Fig. 3, dashed lines), such hydrogen bonding interaction is absent because the benzylic C–H bond and the carbonyl are anti-periplanar.

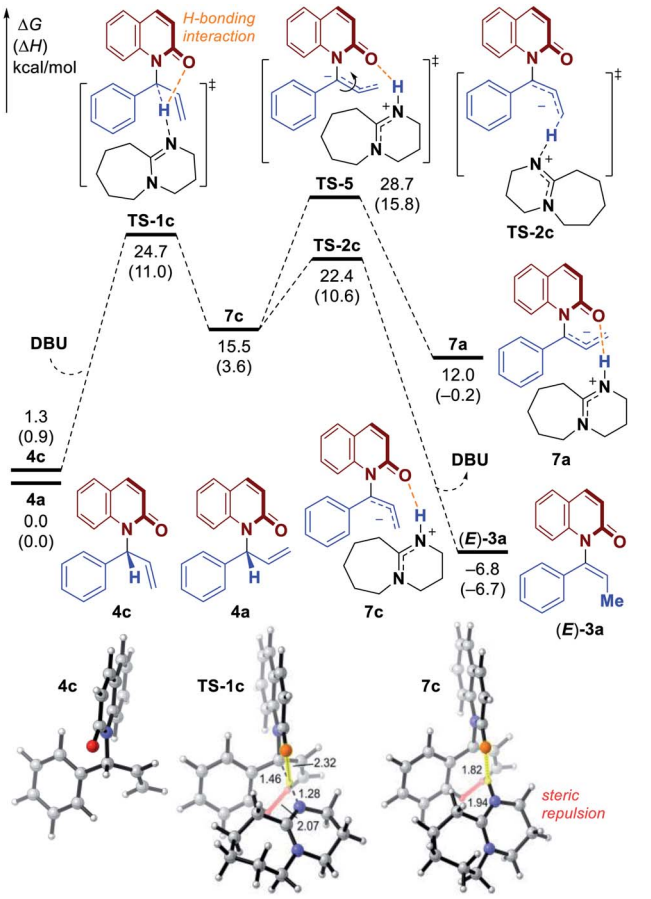

Fig. 4 Free energy profile for the formation of *E*-alkene (*E*)-**3a** through 1,3-H transfer. All energies are calculated at M06-2X/6–311++G(d,p)–SMD(THF)//M06-2X/6-31G(d)–SMD(THF) level of theory.

Moreover, the short H···H distance of 1.95 Å highlighted in **TS-1b** implies the steric repulsion between benzylic and phenyl C–H bonds. Therefore, both **TS-1b** and **7b** are significantly less stable than **TS-1a** and **7a**, respectively. Furthermore, the comparison between **7a** and **7b** implies that the prominent hydrogen bonding interaction could promote the stabilization of **7a** by 5.3 kcal mol^{-1}. Because of the hydrogen bonding and electrostatic attraction (see Fig. S1† for the NCI plot of **7a**), the dissociation of chiral ion-pair **7a** is endergonic by 9.1 kcal mol^{-1} (see Fig. S3† for details), which is consistent with the deuterium labelling experiment (Fig. 2, eqn (3)). From **7a**, racemization *via* C–N bond rotation (**TS-3**) requires a very high barrier. Instead, protonation of the terminal allylic carbon takes place *via* **TS-2a** with an energy barrier of 8.3 kcal mol^{-1}, generating the (*P*)-enantiomer of the enamide product **3a**. This preferred stereochemistry is consistent with the experimental mechanistic studies (Fig. 2). Once **(*P*)-3a** is formed, the racemization to form **(*M*)-3a** requires a high barrier of 27.4 kcal mol^{-1} (*via* **TS-4**), which is consistent with the configurational stability of the product under room temperature.

It should be noted that the high levels of stereospecificity is kinetically controlled, because the less stable conformer **4b**,

which would lead to the unobserved (*M*)-enantiomer of **3a**, is less stable than **4a** by only 1.3 kcal mol^{-1} with an isomerization barrier of 12.0 kcal mol^{-1} (see Fig. S4† for details), indicating a noticeable population of **4b** in the ground state (~10%). Because deprotonation from **4b** is kinetically disfavored, this pathway to form **(*M*)-3a** is completely suppressed.

Based on the experimental results, the atroposelective vinylation products were obtained in high *Z*/*E* ratio (usually >20/1). Our computational studies indicate that the deprotonation of conformer **4c** to form *E*-alkene **(*E*)-3a** has an activation free energy of 24.7 kcal mol^{-1} (**TS-1c**, Fig. 4), which is 2.9 kcal mol^{-1} higher than that of **TS-1a**. The isomerization of **7a** to **7c** (*via* **TS-5**) is found to be endergonic and requires a high barrier. Therefore, the two possible pathways to form **7c** and eventually *E*-alkene **(E)-3a** are both less favorable. Optimized structures show that the **TS-1c** and **7c** are both destabilized by 1,3-allylic strain with the phenyl group – the highlighted H···H distances in **TS-1c** and **7c** (Fig. 4) are only 2.07 and 1.94 Å, respectively.

Based on these studies above, the mechanism and origin of stereoselectivity of [1,3]-H transfer are summarized in Fig. 5. After the enantioenriched allylation product **I** is formed under the classic iridium-catalyzed asymmetric allylic substitution (Fig. 2), the DBU promoted deprotonation of **I** at the benzylic position would occur to generate a chiral ion-pair intermediate **III** through transition state **II-TS**. Both **II-TS** and **III** are stabilized by the H-bonding interaction between the iminium N–H and the amide carbonyl group. As deprotonation is the rate-determining step, subsequent re-protonation of the terminal allylic carbon from **III** could accomplish the [1,3]-H transfer and generate the axially chiral product **(*P*)-IV**. In contrast, the disfavored (*M*)-enantiomer **(*M*)-IV** is generated through the same mechanism from **I-b**, which is a conformer of **I**. The corresponding deprotonation transition state **IIb-TS** is less stable due to the steric repulsion and the absence of H-bonding interaction. Thus, the deprotonation of **I-b** is much slower. Moreover, the racemization of chiral ion-pair **III** and **III-b** is difficult to occur compared with the re-protonation step, which suggests

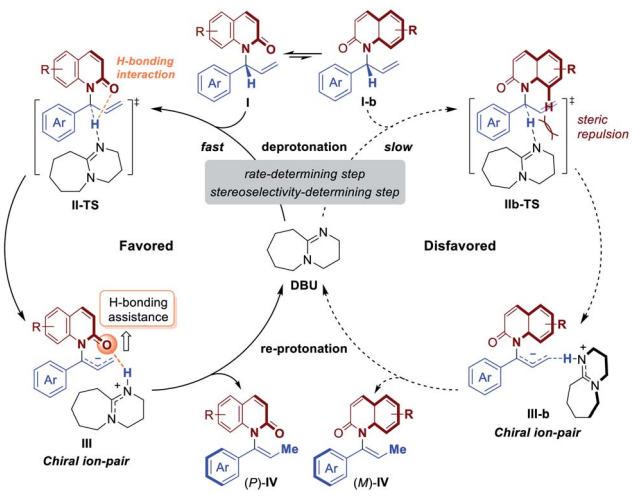

Fig. 5 Proposed mechanism of H-bonding assisted stereospecific [1,]-H transfer process.

Table 3 Axial to central chirality transfer for epoxidation[a]

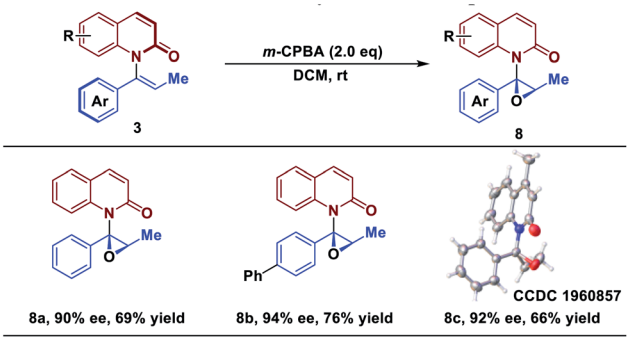

[a] Reaction conditions: all reactions were run on 0.1 mmol scale with respect to **3**. ee determined by chiral HPLC. Isolated yield.

that the deprotonation is also the stereoselectivity-determining step. Therefore, we could draw the conclusion that the stabilizing H-bonding interaction not only facilitates the [1,3]-H transfer but also ensure the high levels of stereospecificity during the central-to-axial chirality transfer.

Axial to central chirality transfer

Catalytic asymmetric epoxidation is a powerful transformation in organic synthesis because the generated optically active epoxides are common motifs in biologically active compounds and biosynthetic intermediates.[50–54] Finally, to demonstrate the utility of the strategy, epoxidations of products **3** were investigated for their stereospecificity. To our delight, treatment of **3** with *m*-CPBA afforded the epoxide scaffolds in good yield, while maintaining the enantiomeric excess (Table 3). The protocol established here represents a novel strategy of asymmetric epoxidation *via* axial-to-central chirality transfer.

Conclusion

In conclusion, we have demonstrated the first example of an atroposelective synthesis of axially chiral enamides bearing the N–C axis. The reaction provides entry to a wide range of quinolone- and pyridone-derived axially chiral enamides in excellent yields with high enantioselectivities. Preliminary mechanistic studies revealed that the reaction proceeds *via* a pathway in which isomerization is the terminal reaction, occurring after the asymmetric allylic amination. Theoretical calculation combined with experimental studies revealed that the isomerization occurs through a hydrogen bonding interaction assisted [1,3]-H transfer, which enantioselectively generates the enamide products. Moreover, the assistance of hydrogen bonding interaction is crucial for the reactivity and stereospecificity during central-to-axial chirality transfer. On one hand, it plays a vital role in stabilizing the deprotonation transition state and the chiral ion-pair intermediate; on the other hand, the lack of hydrogen bonding interaction plus the steric repulsion greatly suppressed the formation of the undesired enantiomer. Furthermore, the epoxidation of axially chiral

enamides promises to serve as a useful approach for the preparation of other chiral derivatives by central-to-axial-to-central chirality transfer sequence. Extension of this methodology to other axially chiral styrenes as well as detailed mechanistic studies is currently underway in our laboratory.

Conflicts of interest

There are no conflicts to declare.

Acknowledgements

We gratefully acknowledge the financial support from the Natural Science Foundation of Jiangsu Province (BK20180447), the Fundamental Research Funds for the Central Universities (30918011313, 30919011404), the NSF (CHE1707490). P. L and X. Q. thank the University of Pittsburgh and the National Science Foundation (CHE-1654122) for financial support of the computational work. DFT calculations were performed at the Center for Research Computing at the University of Pittsburgh, the Texas Advanced Computing Center (TACC) at The University of Texas at Austin, and the Extreme Science and Engineering Discovery Environment (XSEDE) supported by the National Science Foundation grant number ACI-1548562. We especially Prof. Yi-Ming Wang (University of Pittsburgh) for helpful suggestions in the preparation of the manuscript. We also thank Prof. F. Dean Toste (UC Berkeley) and Prof. Hiroshi Naka (Nagoya University) for helpful discussions.

References

1 D. Cahard, S. Gaillard and J.-L. Renaud, *Tetrahedron Lett.*, 2015, **56**, 6159.
2 A. H. Hoveyda, S. J. Malcolmson, S. J. Meek and A. R. Zhugralin, *Angew. Chem., Int. Ed.*, 2010, **49**, 34.
3 E. Larionov, H. Li and C. Mazet, *Chem. Commun.*, 2014, **50**, 9816.
4 Y. Saga, R. Motoki, S. Makino, Y. Shimizu, M. Kanai and M. Shibasaki, *J. Am. Chem. Soc.*, 2010, **132**, 7905.
5 Y. Wu, R. P. Singh and L. Deng, *J. Am. Chem. Soc.*, 2011, **133**, 12458.
6 Y. Wu and L. Deng, *J. Am. Chem. Soc.*, 2012, **134**, 14334.
7 X. Zhou, Y. Wu and L. Deng, *J. Am. Chem. Soc.*, 2016, **138**, 12297.
8 S. Martinez-Erro, A. Sanz-Marco, A. B. Gómez, A. Vázquez-Romero, M. S. G. Ahlquist and B. Martín-Matute, *J. Am. Chem. Soc.*, 2016, **138**, 13408.
9 S. Martinez-Erro, V. García-Vázquez, A. Sanz-Marco and B. Martín-Matute, *Org. Lett.*, 2020, **22**, 4123.
10 N. Molleti, S. Martinez-Erro, A. C. Cerdán, A. Sanz-Marco, E. Gomez-Bengoa and B. Martín-Matute, *ACS Catal.*, 2019, **9**, 9134.
11 J. A. Dabrowski, F. Haeffner and A. H. Hoveyda, *Angew. Chem., Int. Ed.*, 2013, **52**, 7694.
12 V. Bizet, X. Pannecoucke, J.-L. Renaud and D. Cahard, *Angew. Chem., Int. Ed.*, 2012, **51**, 6467.
13 J. C. Golec, E. M. Carter, J. W. Ward, W. G. Whittingham, L. Simón, R. S. Paton and D. J. Dixon, *Angew. Chem., Int. Ed.*, 2020, DOI: 10.1002/anie.202006202.
14 D. M. H. Ascough, F. Duarte and R. S. Paton, *J. Am. Chem. Soc.*, 2018, **140**, 16740.
15 X.-S. Xue, X. Li, A. Yu, C. Yang, C. Song and J.-P. Cheng, *J. Am. Chem. Soc.*, 2013, **135**, 7462.
16 T. Kawabata, K. Yahiro and K. Fuji, *J. Am. Chem. Soc.*, 1991, **113**, 9694.
17 S.-C. Zheng, S. Wu, Q. Zhou, L. W. Chung, L. Ye and B. Tan, *Nat. Commun.*, 2017, **8**, 15238.
18 J. D. Jolliffe, R. J. Armstrong and M. D. Smith, *Nat. Chem.*, 2017, **9**, 558.
19 Y. Tan, S. Jia, F. Hu, Y. Liu, L. Peng, D. Li and H. Yan, *J. Am. Chem. Soc.*, 2018, **140**, 16893.
20 S. Jia, Z. Chen, N. Zhang, Y. Tan, Y. Liu, J. Deng and H. Yan, *J. Am. Chem. Soc.*, 2018, **140**, 7056.
21 J. Feng, B. Li, Y. He and Z. Gu, *Angew. Chem., Int. Ed.*, 2016, **55**, 2186.
22 Y. Liang, J. Ji, X. Zhang, Q. Jiang, J. Luo and X. Zhao, *Angew. Chem., Int. Ed.*, 2020, **59**, 4959.
23 L. Jin, Q.-J. Yao, P.-P. Xie, Y. Li, B.-B. Zhan, Y.-Q. Han, X. Hong and B.-F. Shi, *Chem*, 2020, **6**, 497.
24 S.-L. Li, C. Yang, Q. Wu, H.-L. Zheng, X. Li and J.-P. Cheng, *J. Am. Chem. Soc.*, 2018, **140**, 12836.
25 J.-W. Zhang, J.-H. Xu, D.-J. Cheng, C. Shi, X.-Y. Liu and B. Tan, *Nature Commun*, 2016, **7**, 10677.
26 S. Shirakawa, K. Liu and K. Maruoka, *J. Am. Chem. Soc.*, 2012, **134**, 916.
27 Y. Kikuchi, C. Nakamura, M. Matsuoka, R. Asami and O. Kitagawa, *J. Org. Chem.*, 2019, **84**, 8112.
28 S. Brandes, M. Bella, A. Kjærsgaard and K. A. Jørgensen, *Angew. Chem., Int. Ed.*, 2006, **45**, 1147.
29 F. Eudier, P. Righi, A. Mazzanti, A. Ciogli and G. Bencivenni, *Org. Lett.*, 2015, **17**, 1728.
30 J. Zhang, Y. Zhang, L. Lin, Q. Yao, X. Liu and X. Feng, *Chem. Commun.*, 2015, **51**, 10554.
31 N. Di Iorio, P. Righi, A. Mazzanti, M. Mancinelli, A. Ciogli and G. Bencivenni, *J. Am. Chem. Soc.*, 2014, **136**, 10250.
32 H.-Y. Bai, F.-X. Tan, T.-Q. Liu, G.-D. Zhu, J.-M. Tian, T.-M. Ding, Z.-M. Chen and S.-Y. Zhang, *Nature Commun*, 2019, **10**, 3063.
33 A. J. Clark, D. P. Curran, D. J. Fox, F. Ghelfi, C. S. Guy, B. Hay, N. James, J. M. Phillips, F. Roncaglia, P. B. Sellars, P. Wilson and H. Zhang, *J. Org. Chem.*, 2016, **81**, 5547.
34 R. Takeuchi and S. Kezuka, *Synthesis*, 2006, 3349.
35 J. F. Hartwig and L. M. Stanley, *Acc. Chem. Res.*, 2010, **43**, 1461.
36 P. Tosatti, A. Nelson and S. P. Marsden, *Org. Biomol. Chem.*, 2012, **10**, 3147.
37 X.-J. Liu, C. Zheng, Y.-H. Yang, S. Jin and S.-L. You, *Angew. Chem., Int. Ed.*, 2019, **58**, 10493.
38 J. C. Hethcox, S. E. Shockley and B. M. Stoltz, *ACS Catal.*, 2016, **6**, 6207.
39 J. Qu and G. Helmchen, *Acc. Chem. Res.*, 2017, **50**, 2539.
40 Q. Cheng, H.-F. Tu, C. Zheng, J.-P. Qu, G. Helmchen and S.-L. You, *Chem. Rev.*, 2019, **119**, 1855.

41 S. L. Rössler, D. A. Petrone and E. M. Carreira, *Acc. Chem. Res.*, 2019, **52**, 2657.
42 X. Zhang, Z.-P. Yang, L. Huang and S.-L. You, *Angew. Chem., Int. Ed.*, 2015, **54**, 1873.
43 X.-d. Bai, J. Wang and Y. He, *Adv. Synth. Catal.*, 2019, **361**, 496.
44 For selected example on central-to-axial chirality transfer *via in stiu* isomerization, see: C. Xu, H. Zheng, B. Hu, X. Liu, L. Lin and X. Feng, *Chem. Commun.*, 2017, **53**, 9741.
45 S. Heeb, M. P. Fletcher, S. R. Chhabra, S. P. Diggle, P. Williams and M. Cámara, *FEMS Microbiol. Rev.*, 2011, **35**, 247.
46 J. P. Michael, *Nat. Prod. Rep.*, 2007, **24**, 223.
47 V. Sridharan, P. A. Suryavanshi and J. C. Menéndez, *Chem. Rev.*, 2011, **111**, 7157.
48 It was speculated that catalytic amount TBD play a role of base for construction of **4**. See ESI for more substrate scope.†.
49 Absolute configuration of **4a** was assigned by analogy to that of **4f**, which was determined by comparation of literature (ESI for details†). A. Rodrigues, E. E. Lee and R. A. Batey, *Org. Lett.*, 2010, **12**, 260.
50 T. Katsuki and K. B. Sharpless, *J. Am. Chem. Soc.*, 1980, **102**, 5974.
51 Y. Zhu, Q. Wang, R. G. Cornwall and Y. Shi, *Chem. Rev.*, 2014, **114**, 8199.
52 R. L. Davis, J. Stiller, T. Naicker, H. Jiang and K. A. Jørgensen, *Angew. Chem., Int. Ed.*, 2014, **53**, 7406.
53 Q.-H. Xia, H.-Q. Ge, C.-P. Ye, Z.-M. Liu and K.-X. Su, *Chem. Rev.*, 2005, **105**, 1603.
54 G. D. Faveri, G. Ilyashenko and M. Watkinson, *Chem. Soc. Rev.*, 2011, **40**, 1722.